

SCIENTIFIC REPORTS



OPEN

Extreme decay of meteoric beryllium-10 as a proxy for persistent aridity

Rachel D. Valletta¹, Jane K. Willenbring¹, Adam R. Lewis², Allan C. Ashworth² & Marc Caffee^{3,4}

Received: 26 June 2015

Accepted: 20 October 2015

Published: 09 December 2015

The modern Antarctic Dry Valleys are locked in a hyper-arid, polar climate that enables the East Antarctic Ice Sheet (EAIS) to remain stable, frozen to underlying bedrock. The duration of these dry, cold conditions is a critical prerequisite when modeling the long-term mass balance of the EAIS during past warm climates and is best examined using terrestrial paleoclimatic proxies. Unfortunately, deposits containing such proxies are extremely rare and often difficult to date. Here, we apply a unique dating approach to tundra deposits using concentrations of meteoric beryllium-10 (¹⁰Be) adhered to paleolake sediments from the Friis Hills, central Dry Valleys. We show that lake sediments were emplaced between 14–17.5 My and have remained untouched by meteoric waters since that time. Our results support the notion that the onset of Dry Valleys aridification occurred ~14 My, precluding the possibility of EAIS collapse during Pliocene warming events. Lake fossils indicate that >14 My ago the Dry Valleys hosted a moist tundra that flourished in elevated atmospheric CO₂ (>400 ppm). Thus, Dry Valleys tundra deposits record regional climatic transitions that affect EAIS mass balance, and, in a global paleoclimatic context, these deposits demonstrate how warming induced by 400 ppm CO₂ manifests at high latitudes.

The long-standing dispute concerning the stability of the East Antarctic Ice Sheet (EAIS) calls into question its susceptibility to collapse throughout Neogene climate changes¹. Two opposing views pervade the literature: the “dynamic” hypothesis posits that the EAIS underwent major retraction during mild Pliocene warming events, reducing to as much as two-thirds of its present size^{2–4}, while the opposing “stable” hypothesis argues the EAIS has been largely frozen to its bed since ~14 My and has undergone only minimal, peripheral melting during Pliocene warming^{5–8}. The dynamic theory - if correct - would imply drastic Antarctic ice mass loss and resultant sea-level rise (tens of meters) under atmospheric temperatures and CO₂ concentrations that were only modestly greater than today (2–3 °C and 350–450 ppmv)^{9,10} and that are projected within the coming century¹¹. With such great implications, there remains a need to expand the number of geological datasets that bear on the EAIS’s behavior through time.

Central to the dynamic/stable controversy is the timing of the onset of polar aridity, which limits substantial ice mass loss to only sublimation and is a key factor in determining long term EAIS mass balance¹². The hyper-arid polar conditions of the Dry Valleys have protected inland sites from alteration due to weathering via precipitation or ice melt since the mid-Miocene. As such, these relict landscapes have the potential to record the inception of polar aridity and critically comment on the dynamic/stable debate, but targeted sampling locations that contain paleoclimatic proxies are uncommon and difficult to directly date.

¹Department of Earth and Environmental Science, University of Pennsylvania, Philadelphia, Pennsylvania 19104, USA. ²Department of Geosciences, North Dakota State University, Fargo, North Dakota 58108, USA.

³Department of Physics and Astronomy, PRIME Lab, Purdue University, West Lafayette, Indiana 47907, USA.

⁴Department of Earth, Atmospheric, and Planetary Sciences, Purdue University, West Lafayette, Indiana 47907, USA. Correspondence and requests for materials should be addressed to R.D.V. (email: erosion@sas.upenn.edu)

We present a rare, continuous record of climate change contained within the innermost, highest elevation zone of the Dry Valleys. The Friis Hills, Taylor Valley (800 m above sea level) contains a thick (14 m) series of stacked glacial drifts found interbedded with silty paleolacustrine sediments. These sediments contain a diverse fossil assemblage now extinct in Antarctica including *Nothofagus* (southern beech) wood and leaves¹³. Although brine lakes commonly exist alongside and under Antarctic glaciers under the modern climatic regime¹⁴, the fossils within Paleolake Friis sediments were likely deposited in a semi-permanent proglacial lake on wet, freshwater tundra. Because modern climatic conditions at the Friis Hills are extremely cold (average annual temperature: -22°C) and arid (lows measured $<16\%$ relative humidity)¹⁵, these deposits must archive a period of warmer and wetter climatic conditions. Directly dating these sediments becomes necessary to resolve when tundra-like conditions last prevailed in the upper, inner Dry Valleys.

Meteoric beryllium-10 as an age indicator

To provide chronologic control for the lake sediments we utilize beryllium-10 (^{10}Be) as an isotopic tracer. Cosmic-ray-produced (cosmogenic) ^{10}Be forms in the atmosphere when high-energy neutrons from secondary cosmic rays spall nitrogen and oxygen atoms. This ^{10}Be , denoted meteoric ^{10}Be , exists in the form of ^{10}BeO and $^{10}\text{Be}(\text{OH})_2$ in the atmosphere and quickly adheres to atmospheric aerosols (primarily sulfates)¹⁶. The ^{10}Be -bearing aerosols are then delivered to the Earth's surface through wet (rain) or dry (dust) deposition. Through continued deposition, meteoric ^{10}Be will accumulate at the surface and at depth, as ^{10}Be moves into the soil column via infiltration and clay illuviation¹⁷.

Sediment age model

Concentrations of meteoric ^{10}Be adhered to Paleolake Friis sediments are used to model a minimum age of paleolacustrine deposition. Lebatard *et al.* (ref. 17) first demonstrated that it is possible to date ancient terrestrial deposits with meteoric ^{10}Be if, once buried, sediments remain a closed system. One way to achieve this prerequisite is if meteoric waters do not infiltrate the subsurface. When these conditions are met, the measured ^{10}Be reflects the initial inventory that was present at the time of burial, $[^{10}\text{Be}]_{\text{initial}}$, which is only altered by decay. A hyper-arid climate in the Dry Valleys provides the conditions needed for a closed ^{10}Be system, allowing the use of meteoric ^{10}Be as a chronometer.

To model sediment age, we first determine a range of potential $[^{10}\text{Be}]_{\text{initial}}$. This is possible if we model lake sediments as soil surface sediments that have reached equilibrium between ^{10}Be gain (via deposition) and loss (via erosion and decay). Solving Willenbring and von Blanckenburg's equation for steady state erosion rate (ref. 16, Eq. 21) we estimate a likely range of $[^{10}\text{Be}]_{\text{initial}}$ that was accumulated before burial:

$$[^{10}\text{Be}]_{\text{initial}} = \frac{Q}{\rho E} \quad (1)$$

where Q is flux of ^{10}Be to the Earth's surface ($\text{atoms cm}^{-2} \text{y}^{-1}$), ρ is soil density (1.57g cm^{-3}) and E is erosion rate (cm y^{-1}). We use the ^{10}Be flux calculated for Table Mountain ($3.4 \times 10^3 \text{atoms cm}^{-2} \text{y}^{-1}$)¹⁸, a nearby location that is a suitable representative analog of Friis Hills because comparable arid, windy conditions disallow accumulation of atmospheric aerosols on the earth's surface. To estimate E , we use a range of plausible erosion and total denudation rates obtained independently throughout the Dry Valleys on bedrock and regolith material (Supplementary Table S1).

Once the lake sediments were buried, the $[^{10}\text{Be}]_{\text{initial}}$ began to decay to their current concentration. To determine how long this took, we solve the radioactive decay equation for time, t :

$$N(t) = N_0 e^{-\lambda t} \quad (2)$$

where $N(t)$ is the measured $[^{10}\text{Be}]$ in buried lake sediments (atoms g^{-1}), N_0 is $[^{10}\text{Be}]_{\text{initial}}$ (atoms g^{-1}) determined using Eq. 1, and λ is the ^{10}Be decay constant ($\lambda = \frac{\ln(2)}{t_{1/2}} = 5 \times 10^{-7} \text{y}^{-1}$). Thus, solving Eq. 2 with a range of $[^{10}\text{Be}]_{\text{initial}}$ values yields the time range during which Paleolake Friis sediments were emplaced.

Central to our approach are measurement capabilities. The ^{10}Be concentrations are measured using an accelerator mass spectrometer (AMS); the detection sensitivity is $\sim 10^4 \text{atoms g}^{-1}$. Given the half-life of ^{10}Be ($t_{1/2} = 1.387 \text{My}$)¹⁹, the detection limit corresponds to a maximum age of $\sim 14 \text{My}$. That is, assuming no $[^{10}\text{Be}]$ in the buried lake sediment is lost to erosion, an AMS measurement of $[^{10}\text{Be}]$ within error of $\sim 10^4 \text{atoms g}^{-1}$ indicates a lake sediment age of at least 14 My.

Results

Three samples collected at or below 26 cm depth at the Friis Hills fall below or within the 1- σ uncertainty of "blank" samples (Table 1). These measured concentrations approach the analytical limit of AMS ($^{10}\text{Be}/^9\text{Be} \approx 9 \times 10^{-16}$) and chemical extraction process (ranging from $^{10}\text{Be}/^9\text{Be} \approx 1 \times 10^{-15}$ to 5×10^{-15}). We note that other publications measure concentrations at the surface and at depth up to two and six orders of magnitude greater, respectively^{19,21-23}; see Fig. 1. Higher concentrations may simply be a reflection of younger surfaces. The most comparable measurements made elsewhere are from Table Mountain

Sample	Sample depth (cm)	AMS Be 10/9 (10^{-14} atoms atoms $^{-1}$)	Error (10^{-14} atoms atoms $^{-1}$)	[^{10}Be] (10^5 atoms g $^{-1}$)	1- σ error (10^5 atoms g $^{-1}$)
Friis Hills Pit 1					
ANT-08-FH-03	0	110.0	1.8	150.0	3.0
ANT-08-FH-02	20	2.4	0.24	3.1	0.36
ANT-08-FH-01	60	0.3	0.06	0.03	0.1
Friis Hills Pit 2					
ANT-08-FH-05	26	0.1	0.04	-0.1	0.1
ANT-08-FH-04	30	0.20	0.11	-0.054	0.18
Chemical blanks					
1	N.A.	0.2	0.08	0.3	0.3
2	N.A.	0.2	0.09	0.3	0.3

Table 1. Meteoric ^{10}Be adhered to Paleolake Friis sediments.

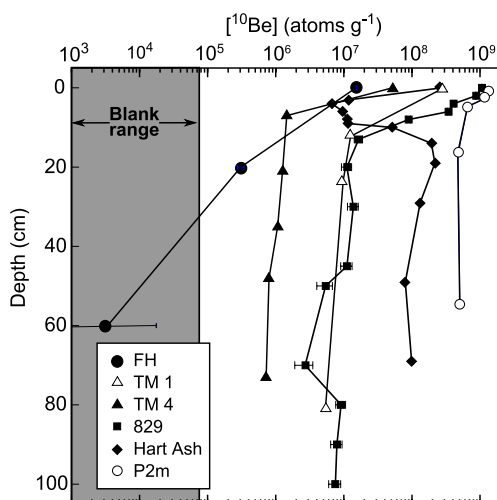


Figure 1. Meteoric [^{10}Be] measured in shallow Dry Valleys sediments: FH (Friis Hills, this study's Pit 1); TM 1, TM 4 (corrected for *in-situ* ^{10}Be contamination)¹⁸; 829²⁰; Hart Ash (and its underlying paleosol)²¹; P2m²². Gray shading indicates measured [^{10}Be] and associated error in the chemical blank. Results from Pit 2 register [^{10}Be] < 0 atoms g $^{-1}$ and, as such, cannot be plotted on log scale.

(Fig. 1, profile TM4). These data have been corrected for contamination from *in situ* ^{10}Be . While meteoric ^{10}Be is adsorbed to the outside of clay minerals, *in situ* ^{10}Be is produced and contained within the mineral structure itself. As Dickinson *et al.* (ref. 20 note, *in situ* concentrations are commonly <1% of the meteoric ^{10}Be concentrations, but because of the great age of Dry Valleys sediments these two fractions may be of the same magnitude. *In situ* ^{10}Be concentrations are most likely liberated via partial decomposition of the clay mineral due to an aggressive leaching solution. By correcting for this contamination, the authors constrain the ^{10}Be flux value (Q) that we use to model the [^{10}Be]_{initial} range.

The modeled [^{10}Be]_{initial} range is 0.83 to 22×10^7 atoms g $^{-1}$ (Supplementary Table S1). We compile a database of [^{10}Be] measurements from modern and ancient lake sediments and find that our estimates are well within the range of published values (Supplementary Table S2). To determine when buried lake sediments were emplaced, we solve Eq. 2 using this [^{10}Be]_{initial} range and $N(t) = 3.48 \times 10^4 \pm 3.48 \times 10^4$ atoms g $^{-1}$, the concentration of the chemical blank used to represent buried lake sediments, to produce a range of 11.0–17.5 My; see Fig. 2. Based on AMS measurement capabilities, lake sediments containing [^{10}Be] within error of the chemical blank are at least 14 My; see above. Accordingly, we raise the lower age limit from 11 My to 14 My. The upper limit of 17.5 My is in agreement with a 19.76 ± 0.11 My ($^{40}\text{Ar}/^{39}\text{Ar}$ dated) ash that lies stratigraphically below sampling Pit 1 to the east²³. The final adjusted age range for the emplacement of Paleolake Friis sediments is 14.0–17.5 My.

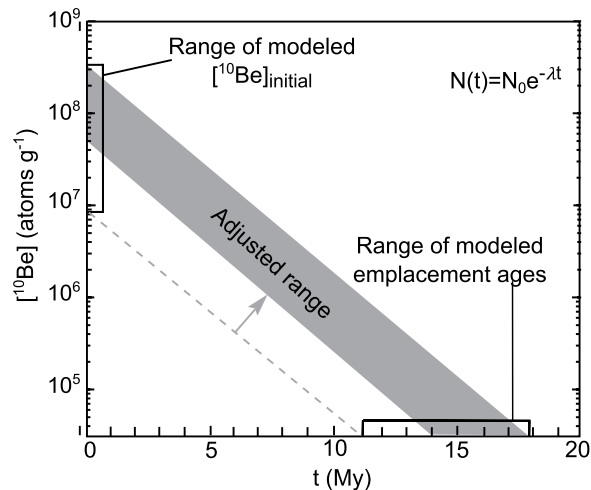


Figure 2. Using the radioactive decay equation, the decay of $[^{10}\text{Be}]_{\text{initial}}$ to the modern “blank” concentration ($3.48 \times 10^4 \pm 3.48 \times 10^4 \text{ atoms g}^{-1}$) corresponds to a sediment emplacement age of 11.0–17.5 My. The AMS detection sensitivity of $\sim 10^4 \text{ atoms g}^{-1}$ corresponds to $\sim 14 \text{ My}$ resulting in an adjusted age range of 14.0–17.5 My.

Middle Miocene climatic transitions & Paleolake Friis emplacement. Lake sediments’ age range spans the Middle Miocene Climatic Optimum (MMCO) $\sim 15\text{--}17 \text{ My}$. This period is characterized by increases in global marine and terrestrial temperatures and reduced global ice coverage as indicated by marine stable isotope records²⁴. In the Ross Sea region, abundant evidence for increased temperatures during the MMCO is well documented in the ANDRILL 2A core, including lithostratigraphic²⁵, palynological²⁶ and leaf wax abundance²⁷ studies. These studies recognize periods of a retracted EAIS margin, decreased sea ice coverage, increased precipitation along the Ross Sea coastline, and a proliferation of vegetation. Definitive terrestrial evidence of the MMCO is found in high altitude tills deposited by wet-based ice²⁸ and in preserved lake fossils⁸, but is otherwise sparse.

The Middle Miocene Climate Transition (MMCT) followed the MMCO at $\sim 14 \text{ My}$. It is marked most notably by ice sheet expansion accompanied by a rapid, 8°C cooling on land ($14.07\text{--}13.85 \text{ My}$)⁸ and $6\text{--}7^\circ\text{C}$ cooling in the southern Pacific ocean ($14.2\text{--}13.8 \text{ My}$)²⁹. Marine depositional and terrestrial erosional features record this expansion in thick offshore Middle Miocene units in the Ross Sea³⁰, in the cross-cutting bedrock channels of the Labyrinth, Wright Valley³¹, and in the Friis Hills themselves, where glacial expansion and down-cutting likely formed the near-modern surface²³. A synchronized transition to arid conditions is recorded in volcanic ashes in nearby Olympus²⁸ and western Asgard Ranges^{5,6}. Workers note that ashfalls infill sand-wedge troughs, which form only in cold/dry conditions, contain glass shards, and lack evidence of cryoturbation or clay formation. This pristine preservation indicates no presence of surface moisture or chemical weathering since the time of ash emplacement. The oldest, unaltered ash deposits in the Dry Valleys indicate that other parts of the region have experienced uninterrupted polar desert climate since $\sim 15 \text{ My}$ ³; our results expand this zone.

Based on the abundant evidence for warmer global and regional temperatures $\sim 15\text{--}17 \text{ My}$, we suggest that Paleolake Friis sediments were likely emplaced during the MMCO (Fig. 3). At their warmest, terrestrial summer temperatures reached as high as 10°C ²⁶, great enough to support a wet tundra environment in which fossils like *Nothofagus* thrived [ref. 4 associated this species with mean summer temperatures of $\sim 5^\circ\text{C}$]. Warmer temperatures coincide with increases in global CO_2 reconstructions. According to Royer’s data compilation⁹ the MMCO is arguably the last time global CO_2 remained $>400 \text{ ppm}$ for several million years, making CO_2 a possible driver of EAIS retraction and terrestrial plant proliferation at this time. The linkages between global CO_2 concentrations, ice volume and vegetation during the MMCO have proven challenging to model, but these simulations are valuable towards our understanding of future climate and require improvement. A notable model deficiency is the lack of reliable temperature proxy data, particularly at high latitudes (e.g. ref. 32). The Paleolake Friis deposits, along with those described in Lewis *et al.* (ref. 8), represent the southernmost terrestrial deposits, and highest latitude deposits overall, available for middle Miocene paleoclimatic reconstructions. These records should be incorporated as constraints when modeling the MMCO; they are especially useful in reconstructing Equator to pole temperature gradients.

Following their deposition, Paleolake Friis sediments entered a closed system, one that did not receive meteoric ^{10}Be in surface waters via ice melt or precipitation. This closed system is maintained if plunging temperatures of the MMCT $\sim 14 \text{ My}$ were accompanied by an onset of extreme aridity. The lack of ^{10}Be

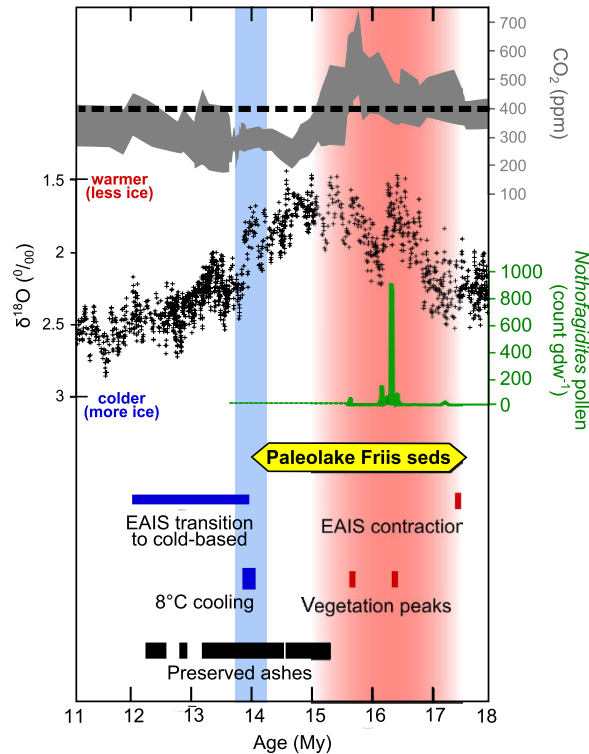


Figure 3. Modeled age range of Paleolake Friis sediments (14.0 to 17.5 My) and global and regional paleoclimatic indicators throughout the middle Miocene. In red: the MMCO defined globally ~15–17 My²⁴ and regionally 15.4–17.6 My²⁵. In blue: the MMCT, 13.8–14.2 My²⁹. Labeled events include: the onset of EAIS contraction, 17.21–17.49 My³⁵; peaks in vegetation expansion (including terrestrial tundra taxa and marine and freshwater algae species) centered on 15.7 and 16.4 My²⁷; the range of ages of pristinely preserved ashes (measurement error included in bar width)^{5,6,28}; 8 °C cooling on Antarctica⁸; EAIS transition to cold-based 12–14 My prior to major expansion at ~12 My^{8,24}. Black crosses: global $\delta^{18}\text{O}$ record (‰), five point smooth²⁴. Grey shading: global atmospheric CO_2 (ppm) reconstruction, 5 point smooth⁹. Green line: *Nothofagidites* (type *Nothofagus fusca*) pollen abundance (count per grams dry weight, gdw^{-1}) measured in AND-2A core²⁷. The pollen abundance peak ~16.4 My is further evidence that *Nothofagus*, those leaf fossils in Paleolake Friis sediments, existed on Antarctica during the MMCO. The dotted green line represents a sedimentary hiatus in the AND-2A core that is attributed to ice sheet growth.

in lake sediments indicates persistent polar aridity was established in the inner Dry Valleys by at least this time, contradicting the notion of large-scale EAIS collapse during the Pliocene.

Methods

Treating paleolake sediments. During the austral summer of 2008, five samples for meteoric ^{10}Be dating were collected from silty paleolacustrine sediments exposed on a hillside within the Friis Hills stacked tills. Samples were prepared at the University of Pennsylvania Cosmogenic Isotope Lab following protocol for adhered meteoric ^{10}Be extraction, including a 0.5 M HCl agitated leach and a 1 M hydroxylamine hydrochloride ($\text{NH}_2\text{OH}\cdot\text{HCl}$) leach in an ultrasonic bath³³. Following ^9Be spike addition (GFZ German Research Centre for Geosciences “Phenakite” standard, $^{10}\text{Be}/^9\text{Be}_{\text{spike}} = 10^{-16}$) and ion exchange chromatography, samples were oxidized over open flame, packed with Nb powder into cathode targets, and sent to the Purdue PRIME Lab for AMS measurement of $^{10}\text{Be}/^9\text{Be}$.

Error assessment. The overall range of erosion rates reported in the literature is 0.1–2.6 m My^{-1} corresponding to an overall range of $[\text{}^{10}\text{Be}]_{\text{initial}}$ of $0.83\text{--}22 \times 10^7$ atoms g^{-1} . Not all published erosion rates are reported with associated errors and cannot be recalculated because in most cases erosion rate error distributions, ^9Be carrier spike, and/or assumed $^{10}\text{Be}/^9\text{Be}$ spike ratio were not reported. These missing data prohibit the inclusion of simple error propagation in our age model. Nevertheless, to assess the impact of error on our age estimates we apply a commonly reported error value of 10% to the upper and lower erosion rate estimates. This implementation results in marginally different lake sediment age estimates (10.7–17.7 My). Thus, incorporating erosion rate error does not affect our overall thesis that sediments were emplaced during the MMCO.

Choosing a flux value, Q. The proper choice of a flux value, Q, is critical for constraining the emplacement age of Friis Hills sediments. We have chosen a relatively low flux value of 3.4×10^3 atoms $\text{cm}^{-2} \text{y}^{-1}$ because it was quantified from a nearby location with extremely similar climatic and erosional conditions¹⁹. Other applications of meteoric ¹⁰Be dating in the Dry Valleys have instead used a higher flux value that was determined from ¹⁰Be accumulated in the Taylor Dome ice core (1.3×10^5 atoms $\text{g}^{-1} \text{y}^{-1}$)³⁴. Using this greater flux value for Paleolake Friis sediments yields a much older emplacement age of 18.2–24.8 My. This range exceeds the underlying ash's age of 19.76 My¹². As such, we regard the Taylor Dome flux value as unreasonably high for the Friis Hills location.

References

- Barrett, P. J. Resolving views on Antarctic Neogene glacial history—the Sirius debate. *Earth Environ. Sci. Trans. R. Soc. Edinburg* **104**, 31–53 (2013).
- Wilson, G. S. The Neogene East Antarctic Ice Sheet: A dynamic or stable feature? *Quat. Sci. Rev.* **14**(2), 101–123 (1995).
- Hambrey, M. J. & McKelvey, B. Major Neogene fluctuations of the East Antarctic ice sheet: Stratigraphic evidence from the Lambert Glacier region. *Geology* **28**(10), 887 (2000).
- Rebesco, M., Camerlenghi, A., Geletti, R. & Canals, M. Margin architecture reveals the transition to the modern Antarctic ice sheet ca. 3 My. *Geology* **34**(4), 301 (2006).
- Marchant, D. R., Denton, G. H., Sugden, D. E. & Swisher, C. C., III. Miocene glacial stratigraphy and landscape evolution of the western Asgard Range, Antarctica. *Geog. Ann. A* **75**(4), 303–330 (1993).
- Marchant, D. R., Denton, G. H., Swisher, C. C., III & Potter, N., Jr. Late Cenozoic Antarctic paleoclimate reconstructed from volcanic ashes in the Dry Valleys region of southern Victoria Land. *Geol. Soc. Am. Bull.* **108**(2), 181–194 (1996).
- Sugden, D. The East Antarctic Ice Sheet: unstable ice or unstable ideas? *T. I. Brit. Geog.* **21**, 443–454 (1996).
- Lewis, A. R. *et al.* Mid-Miocene cooling and the extinction of tundra in continental Antarctica. *P. Natl. Acad. Sci. USA* **105**(31), 10676–10680 (2008).
- Royer, D. L. Atmospheric CO₂ and O₂ during the Phanerozoic: Tools, patterns, and impacts. In *Treatise on Geochemistry* 6 (ed. Farquhar, J.), 251–267 (Oxford, UK, Elsevier, 2014).
- Dowsett, H. J. The PRISM palaeoclimate reconstruction and Pliocene sea-surface temperature. In *Deep-time perspectives on climate change: Marrying the signal from computer models and biological proxies* (eds Williams, M., Haywood, A. M., Gregory, J. & Schmidt, D. N.), 459–480 (Micropalaeontological Society Special Publication: London, Geological Society of London, 2007).
- IPCC. *Climate Change 2013: The Physical Science Basis* (Cambridge Univ. Press, 2013).
- Lewis, A. R., Ashworth, A. C. An early to middle Miocene record of ice-sheet and landscape evolution from the Friis Hills, Antarctica. *Geol. Soc. Am. Bull.* doi: 10.1130/B31319.1 (in press).
- Frezzotti, M. *et al.* New estimations of precipitation and surface sublimation in East Antarctica from snow accumulation measurements. *Clim. Dynam.* **23**(7–8), 803–813 (2004).
- Mikucki, J. A. *et al.* Deep groundwater and potential subsurface habitats beneath an Antarctic dry valley. *Nat. Comm.* **6** (2015).
- Fountain, A. Friis Hills Meteorological Station Measurements: knb-lter-mcm.7017.2. (2010) (<http://mcm.lternet.edu/content/friis-hills-meteorological-station-measurements>). Accessed: 08/08/2013.
- Lal, D. & Peters, B. Cosmic ray produced radioactivity on the Earth. *Handbuch der Physik* **46**, 551–612 (1967).
- Willenbring, J. K. & von Blanckenburg, F. Meteoric cosmogenic beryllium-10 adsorbed to river sediment and soil: Applications for Earth-surface dynamics. *Earth-Sci. Rev.* **98**, 105–122 (2010).
- Lebatard, A. E. *et al.* Application of the authigenic ¹⁰Be/⁹Be dating method to continental sediments: reconstruction of the Mio-Pleistocene sedimentary sequence in the early hominid fossiliferous areas of the northern Chad Basin. *Earth Planet. Sc. Lett.* **297**, 57–70 (2010).
- Dickinson, W. W., Schiller, M., Ditchburn, B. G., Graham, I. J. & Zondervan, A. Meteoric Be-10 from Sirius Group suggest high elevation McMurdo Dry Valleys permanently frozen since 6 My. *Earth Planet Sc. Lett.* **355**, 13–19 (2012).
- Chmleff, J., von Blanckenburg, F., Kossert, K. & Jakob, D. Determination of the ¹⁰Be half-life by multicollector ICP-MS and liquid scintillation counting. *Nucl. Instrum. Meth. B* **268**(2), 192–199 (2009).
- Graham, I. J. *et al.* Dating Antarctic soils using atmosphere-derived ¹⁰Be and nitrate. In Gamble, J., Skinner, D., Henrys, S. (Eds.), Antarctica at the Close of a Millennium, *Roy. Soc. New Zealand Bull.* **35**, 429–436 (2002).
- Schiller, M., Dickinson, W., Ditchburn, R. G., Graham, I. J. & Zondervan, A. Atmospheric ¹⁰Be in an Antarctic soil: Implications for climate change. *J. Geophys. Res.* **114**(F01033) (2009).
- Schiller, M., Dickinson, W., Zondervan, A., Ditchburn, R. & Wang, N. Rapid soil accumulation in a frozen landscape. *Geology* **42**(4), 335–338 (2014).
- Zachos, C. Z., Dickens, G. R. & Zeebe, R. E. An early Cenozoic perspective on greenhouse warming and carbon-cycle dynamics. *Nature* **451**(7176), 279–283 (2008).
- Passchier, S. *et al.* Early and middle Miocene Antarctic glacial history from the sedimentary facies distribution in the AND-2A drill hole, Ross Sea, Antarctica. *Geol. Soc. Am. Bull.* **123**(11–12), 2352–2365 (2011).
- Warny, S. *et al.* Palynomorphs from a sediment core reveal a sudden remarkably warm Antarctica during the middle Miocene. *Geology* **37**(10), 955–958 (2009).
- Feakins, S. J., Warny, S. & Lee, J. E. Hydrological cycling over Antarctica during the middle Miocene warming. *Nature Geosci.* **5**(8), 557–560 (2012).
- Lewis, A. R., Marchant, D. R., Ashworth, A. C., Hemming, S. R. & Machlus, M. L. Major middle Miocene global climate change Evidence from East Antarctica and the Transantarctic Mountains. *Geol. Soc. Am. Bull.* **119**(11–12), 1449–1461 (2007).
- Shevenell, A. E., Kennett, J. P. & Lea, D. W. Middle Miocene Southern Ocean Cooling and Antarctic Cryosphere Expansion. *Science* **305**(5691), 1766–1770 (2004).
- Fielding, C. R. *et al.* Sequence stratigraphy of the ANDRILL AND-2A drillcore, Antarctica: A long-term ice-proximal record of Early to Mid-Miocene climate, sea-level and glacial dynamism. *Palaeogeogr. Palaeoclimatol.* **305**(1–4), 337–351 (2011).
- Lewis, A. R., Marchant, D. R., Kowalewski, D. E., Baldwin, S. L. & Webb, L. E. The age and origin of the Labyrinth, western Dry Valleys, Antarctica: Evidence for extensive middle Miocene subglacial floods and freshwater discharge to the Southern Ocean. *Geology* **34**(7), 513–516 (2006).
- Goldner, A., Herold, N. & Huber, M. The challenge of simulating the warmth of the mid-Miocene climatic optimum in CESM1. *Clim. Past* **10**(2), 523–536 (2014).
- Ebert, K., Willenbring, J., Norton, K. P., Hall, A. & Hättestrand, C. Meteoric ¹⁰Be concentrations from saprolite and till in northern Sweden: Implications for glacial erosion and age. *Quat. Geochron.* **12**, 11–22 (2012).
- Steig, E. J. *et al.* Wisconsinian and Holocene climate history from an ice core at Taylor Dome, western Ross embayment, Antarctica. *Geog. Ann. A* **82**(2–3), 213–235 (2000).

35. Sandroni, S. & Talarico, F. M. The record of Miocene climatic events in AND-2A drill core (Antarctica): Insights from provenance analyses of basement clasts. *Global Planet. Change* **75**(1), 31–46 (2011).

Acknowledgements

This research was supported by the University of Pennsylvania, the North Dakota State University and the National Science Foundation (USA) awards 0739693 to ARL and ACA and 1043554 to JKW. PRIME Lab is funded in part by NSF award 1153689. Imagery is provided by the Polar Geospatial Center at the University of Minnesota.

Author Contributions

R.D.V. and J.K.W. performed data analysis, designed the age model, and wrote the manuscript. J.K.W., A.R.L. and A.C.A. designed the field campaign and collected samples. M.C. performed AMS measurements on samples. J.K.W. performed the data analyses. All authors reviewed the manuscript.

Additional Information

Supplementary information accompanies this paper at <http://www.nature.com/srep>

Competing financial interests: The authors declare no competing financial interests.

How to cite this article: Valletta, R. D. *et al.* Extreme decay of meteoric beryllium-10 as a proxy for persistent aridity. *Sci. Rep.* **5**, 17813; doi: 10.1038/srep17813 (2015).



This work is licensed under a Creative Commons Attribution 4.0 International License. The images or other third party material in this article are included in the article's Creative Commons license, unless indicated otherwise in the credit line; if the material is not included under the Creative Commons license, users will need to obtain permission from the license holder to reproduce the material. To view a copy of this license, visit <http://creativecommons.org/licenses/by/4.0/>